Numerical Methods in Civil Engineering, 9-2 (2024) 71-85

Numerical Methods in Civil Engineering

Journal Homepage: https://nmce.kntu.ac.ir/

A Novel Hybrid Meta-Heuristic Algorithm for Optimum High Performance-Based Seismic Designs (HPBSDs) of Steel Shear Walls (SSWs)

Behzad Eftekhar [*], Omid Rezayfar [**]

ARTICLE INFO

RESEARCH PAPER

Article history:
Received:
September 2021
Revised:
December 2024
Accepted:
December 2024

Keywords:
Optimum High Performance-Based Seismic Design (OHPBSD),
Harmony Search (HS),
Steel Shear Wall (SSW),
Multi-Design Variable Configuration (Multi-DVC),
Upper Bound Strategy (UBS)

Abstract

Steel Shear Walls (SSWs) exhibit suitable stiffness among various lateral force-resisting systems, and their application has been extended to tall buildings. In this research, the optimization of a High Performance-Based Seismic Design (HPBSD) of SSWs was introduced using a new optimization method. A hybrid algorithm was developed based on the Harmony Search (HS) algorithm, Multi-Design Variable Configuration (Multi-DVC) cascade optimization, and Upper-Bound Strategy (UBS). This new approach, termed MDVC-UHS, utilized cascade structural sizing optimization to manage numerous variables through a series of DVCs. The UBS was employed to reduce computational time, while the HS was used for global optimization. The MDVC-UHS algorithm was applied to optimize the dimensions of the steel shear wall following high performance-based seismic design principles. The research indicated that as the length of the SSW increased relative to its height, the more it was in the shear mode and the more usage it could have.

1. Introduction

Steel shear walls (SSWs) have been considered for reducing lateral forces from earthquakes and lateral wind forces in buildings, especially tall buildings, over the past three decades. This modern phenomenon, which is rapidly increasing worldwide, is used to build new structures and strengthen existing ones, particularly in earthquake-prone countries such as Japan and the United States. SSWs are a better and faster alternative from an executive perspective and reliable resistance and conduction side not only in steel structures but also in concrete structures.

SSWs are made of steel sheets covered with beams and columns. These walls act like cantilevered sheet metal beams, in which the supports serve as flanges, the beams on the floors serve as stiffeners and steel sheets serve as beam webs. In this system, the connections between beams and columns are fixed connections, and unlike the beam plates where flanges do not play an important role in force reduction due to their weaknesses, columns can play a crucial role in SSWs given their strengths.

The steel sheets can be reinforced with vertical and horizontal hardeners to avoid buckling, especially in the elastic zones. Given the high strength of steel sheets and the utilization of their resistance to buckling even with long SSWs and high shear forces, thin steel sheets can be used. To avoid buckling due to operational loads and instead of increasing the thickness of the sheets, which would be quite uneconomical, stiffeners can be used to strengthen them. Reinforcing the sheets not only prevents buckling due to operational loads but also improves their behavior, especially in their plastic zones.

[*] *Assistant Professor, Department of Civil Engineering, Islamic Azad University Branch Larestan, Larestan, Iran*
[**] *Corresponding author: Professor, Department of Civil Engineering, Semnan University, Semnan, Iran*

https://doi.org/10.61186/NMCE.653.1

The basic idea behind SSWs, which has received considerable attention in recent decades, is the use of a diagonal stress field that arises in them after the steel sheets are buckled. A few years earlier they were used in a limited number of buildings with high-strength steel panels to prevent them from buckling, taking a cue from the shipbuilding industry.

Seismic design of structures is traditionally carried out based on their strengths. Although the structures were designed based on the criteria of existing seismic designs, they suffered significant damage from recent earthquakes. Accordingly, it is necessary to provide performance-based seismic design (PBSD) to achieve better performance and less damage. In recent years, in addition to the assessment and reconstruction of existing buildings, various instructions have been presented on the introduction of the PBSD concepts as well as the design and analysis of the new buildings.

Immediate Occupancy (IO), Life Safety (LS), and Collapse Threshold (CP) were defined as optimized performance levels of structural PBSDs in earthquake engineering. At the IO level, the structure experiences very little damage and has optimal efficiency for continuous use. At the LS level, residents have the opportunity to safely leave the building even after significant damage. The CP level indicates structural collapse caused by increased stress or deflection due to widespread deformation of nonelastic structural members.

Nonlinear analysis tools are used to examine different performance levels of structures during an earthquake. In this area, pushover analysis (PA) has been widely established as an effective tool. The primary and general assessment of structural strength and deformability are the objectives of nonlinear static pushover analysis (NSP), the result of which is the construction of capacity curves of inelastic structures.

Nature is a great source of phenomena that can be modeled to solve engineering problems. Typically, researchers use the laws of nature to solve various engineering problems such as optimization. These include the Evolutionary Algorithm (EA), which was first used by Holand [1], and the Genetic Algorithm (GA), which was adopted from biological evolution and introduced by De Jong [2]. Researchers studying animal social behavior have drawn inspiration from methods such as those of Dorigo et al. and Eberhart et al. were developed the Ant Colony Algorithm (ACO) [3] and the Particle Swarm Optimization (PSO) [4], respectively. Optimization theory has also taken inspiration from the laws of nature through the Gravitational Search Algorithm (GSA) based on physical phenomena, the Harmony Search (HS), the Jaya algorithm, the Gray Wolf Optimization (GWO) algorithm, and the Multi Objective learning-based optimization algorithm introduced by Rashedi et al. [5], Lee and Geem [6], Grzywinski et al. [7], Kalemci et al. [8] and Eirgash [9] respectively.

This newly introduced MDVC-UHS algorithm consists of Multi-Design Variable Configuration (Multi-DVC) [10] and Upper Bound Strategy (UBS) [11] for general optimization of the large-scale structures. The HS method is used for general optimization and the Multi-DVC algorithm is used to control a large amount of the design variables.

The HS algorithm is one of the metaheuristic optimization methods, which is adjusted based on the theory of music composition. This method does not use complex mathematical relationships to generate solutions related to the design variables in each problem and applies a harmony memory containing some of the best solutions each time the optimization process is performed. This mechanism in the HS method ensures that the values of the solutions do not go beyond the boundaries of the search space defined for them and there is no need to update these types of solutions that are constantly generated in other algorithms. Since updating these crowded solutions is a time-consuming process, using the HS method as the main optimization operator in creating solutions has resulted in good convergence speed in reaching the optimal solution in the MDVC-UHS method.

In this new method, a balance between the amount and variety of design variables can be achieved by controlling the structural weight. For this purpose, a configuration that deviates from the design variables is used in each phase of the optimization. By using the optimal design achieved in the previous phase, a new optimization phase can be initiated in parallel with the previous phase. The best design variable configuration, Multi-DVC, performs the first and last stages of optimization, respectively. Nevertheless, optimizing the structures with various design analyses requires a significant amount of time to carry out the calculation. To solve this problem, some non-essential structural analysis can be avoided during optimization using the UBS strategy. Therefore, this recently proposed approach attempted to achieve a generally optimal response with fewer repetitions than the existing algorithmic approach.

In this research, a well-organized optimal seismic design of SSW is presented. Pushover analysis is used to evaluate the structural responses under seismic excitation. This research aims to achieve the minimum structural steel volume resulting in low cost by optimizing the cross-sectional properties for the SSW. The inter–storey drifts were limited to the LS level by designing the design's performance-based pressures. Since effectiveness is important, the sensitivities of an effective method were determined by selecting a gradient-based optimization method as well as complementary and analytical approaches.

2. Performance-based System optimization

This draft rule is necessary to evaluate two factors that must be checked in the event of deflection: the structural strength in the limit state and the serviceability. To design new buildings based on existing building design regulations, the PBSD method is used, which is intended to be different from other seismic design methods. This design method is used to confirm reliable seismic levels that can be used to predict the service life of the structure as it can determine seismic requirements at predefined performance levels, allowing structure designs to be verified at higher seismic performance.

The performance aims to determine their level at a given level of danger. Performance objectives are defined by selecting the performance level of a structure and determining the corresponding seismic hazard level. According to FEMA-273 [12], the power levels LS, IO, and CP mentioned were taken into account in the current research. Each target was associated with a recovery probability of 50 years.

IO, LS, and CP performance levels are commonly assumed at 50, 10, and 2%, respectively, with the probability of exceedance over 50 years [13]. These risk levels were also taken into account in this study.

As another part of PBSD, structural analysis can evaluate structural capacity. The maximum values of inter-storey drifts correspond to this capacity. In the present research, NSP analysis is used to determine the nonlinear structural responses induced by earthquakes. In addition, the displacement coefficient method, adopted from the various static pushover analyses, evaluates the seismic requirements on the building frames under corresponding static earthquake loading [14]. In this procedure, lateral loads have been particularly distributed up until reaching the target displacement; according to FEMA-356 [14] its value can be as follows:

$$\delta_t = C_0 C_1 C_2 C_3 S_a \frac{T_e^2}{4\pi^2} g \quad (1)$$

C_0 relate to the specific and expected maximum inelastic displacements of the probable building; furthermore, displacements for a linear elastic response are measured by C_1. C_2 is used to show the effects of hysteresis shape on the maximum displacement response and C_3 shows the influence of P-Δ. T_e indicates the effective fundamental period of the building in the direction under consideration; In addition, Sa means the acceleration of the response spectrum corresponding to T_e.

The values of the parameters given in Table 1 are used to calculate the spectral acceleration (S_a) for each hazard level. 1 [13]. In this table, the short period is shown as S_S, which is the reaction acceleration parameter for the first second. In addition, the location coefficients are shown as F_a and F_v. In this research, the OpenSees [15] platform performs the pushover analyses.

Table 1: Site parameters at the performance level for the site class of D [13].

Performance level	Hazard level	$_s$ (g)	$_1$ (g)	$_a$	$_v$
IO	0%/50-years	.658	.198	.27	.00
LS	0%/50-years	.794	.237	.18	.92
CP	%/50-years	.150	.346	.04	.70

3. Problem Formulation

The PBSO problem of steel structure should be defined by objective functional and design constraints. In the present study, the objective function is the minimized overall structure weight according to Eq. 2, which defines the objective function as follows:

$$W(X) = \sum_{i=1}^{nm} \rho_i V_i \quad (2)$$

In the above formulary, W stands for structural weight; ρ_i is the weight density, and V_i shows i^{th} member value. Finally, the number of members is displayed in nm. In addition, to ensure optimal performance of the resulting designs, some limitations based on the code used in the design process should be taken into account in the following two steps.

3.1. Relations governing the steel shear wall design

Two general methods for analyzing and designing steel shear walls have been defined so far. The first method was first introduced in the 1980s by Kulak [16], based on studies and research from the University of Alberta in Canada. In this method, the steel sheet is moved through a series of diagonal tendons, and the analysis system is finally designed. The above method registered in the Canadian Building Code has never been used for steel shear walls with thin steel plates, not for steel shear walls with thick steel plates, and not for reinforced steel shear walls. There is also no solution for the analysis and design of the system if the steel shear walls have an opening. This method analyzes the replacement of sheet steel with several bars, sheets, and frames at the same time. Therefore, the designer has no physical idea of the system behavior, especially in plate-frame interaction.

Saburi et al. [17] presented an advanced method in the late 1980s in which attempts were made to respond to all the different situations of the system, either the steel shear walls

with thick and thin steel sheets or the steel shear walls with opening and reinforcement. In addition, the behavior and function of the steel sheet and frame as well as their interaction are monitored separately; which plays an important role in the behavior of the system and can be explained physically.

The panel load shear of each floor can be calculated in this manner by determining the shear force of the floors and the amount of lateral load applied to the steel shear walls. Each of the shear panels of the floor and consequently steel shear walls are analyzable and can be designed.

First step: Pre-buckling stage:

Before buckling of the steel sheet, the stress situations are in a way that the main equal tensile stress and compression stress established along the $45°$ and $135°$, until they achieve to critical buckling stress. The steel sheet critical stress can be calculated by classic steady state theory supposing the simple support. If the steel sheet is thick critical shear stress (τ_{cr}) exceeds the yield shear stress based on Von Mises yield criterion, and the steel sheet theoretically yields, as a result.

$$\tau_{cr} = \frac{K\pi^2 E}{12(1-\mu^2)}\left(\frac{t}{b}\right) \le \frac{\sigma_0}{\sqrt{3}} \tag{3}$$

$$K = 3.35 + 4\left(\frac{b}{d}\right)^2 \qquad for \quad \frac{b}{d} \ge 1 \tag{4}$$

$$K = 5.35\left(\frac{b}{d}\right)^2 + 4 \qquad for \quad \frac{b}{d} \le 1 \tag{5}$$

Where t is the steel sheet thickness, E is the elasticity modulus, μ is the Poisson's ratio, b is the span, d is the panel height and σ_0 is the steel sheet yield stress in the uni-axial tension test of the steel sheet.

The structural capacity is estimated by the nonlinear pushover analysis and the method of displacement coefficient at the LS level of performance. This capacity relates to the maximum values of inter-storey drifts. The second step involves the following constraints:

Second Step: The constraints of post- buckling stage

If the steel plate is thin and buckles before yielding, the sheet cannot bear more compression stress; although compression stress can increase until the steel sheet yields. Therefore, after buckling the sheet by gradually making the tension field and its propagation to all its levels, again load-carrying mechanism will be created called post-buckling. Columns should have sufficient stiffness to diffuse to all its levels, the tension field achieved from the steel sheet. Therefore, the following constraints should be met to be sure that the columns can bear the forces created because of the tension field after buckling the sheet and plastic moment won't be created in them before yielding the mentioned sheet.

$$M_{fp} > \frac{\sigma_{ty} t d^2}{8} \tag{6}$$

Regarding the storey's beam in the steel shear walls, forces inflicted on the link beams from the steel plates of the two adjacent storeys will get neutralized due to slight differences. Therefore, the following Eq. 7 should be considered to provide the stiffness for them, just for the last beams which only withstand the forces inflicted from one steel sheet.

$$M_{sp} > \frac{\sigma_{ty} t b^2}{16} \tag{7}$$

Where M_{sp} is the plastic moment of the last beam.

The constraints of the lateral drifts at the different levels of performance are defined as follows:

$$\theta_k^i \le \theta_{all}^i, \quad k = 1, 2, \ldots, ns, \quad i = LS \tag{8}$$

where θ_k^i is the drift of the k^{th} storey related to a steel structure frame, and the LS level of performance squires the steel structure frame. In this meaning, θ_{all}^i shows the value allowed for them. In this research, this equal value was elected to be 0.2 [18].

4. Proposed Method

To deal with a large number of variables, the following steps introduce the MDVC-UHS algorithm which is made of Multi-DVC cascade optimization. HS acts as the main mechanism of optimization and UBS decreases the computational time.

Step 1: Randomly generate a certain number of primitive solution candidates based on DVCs for design variables. After a series of DVCs are created and categorized in increasing order of magnitude, the coarsest DVC in the primary state is used. This configuration of the cascade mechanism is the principle of random distribution of the first locations of all particles. By defining the design variables, a set of primitive solution candidates could be created according to the following formula and based on the constraints associated with the solution candidate:

$$t_i = t_{\min} + Rand(t_{\max} - t_{\min}) \tag{9}$$

$$b_i = b_{\min} + Rand(b_{\max} - b_{\min}) \tag{10}$$

$$d_i = d_{\min} + Rand(d_{\max} - d_{\min}) \tag{11}$$

In addition, the number of solution vectors in the harmony memory (HMS), i.e. the size of the harmony memory matrix, the harmony consideration rate (HMCR), the pitch adjustment rate (PAR), and the maximum number of

searches are also selected in this step. In the HS algorithm, the HM stores the feasible vectors, all of which lie in the feasible space. The size of Harmony memory determines the number of vectors to be stored.

Step 2: Analyze the structure considering the number of design variables present in a candidate solution and considering the penalty functions and fitness functions for each candidate solution.

According to the following relationship, the degree of fitness value could be calculated and also categorized based on the lowest fitness for each candidate solution. The lowest fitness function could be introduced as the optimal response. There are usually different approaches to calculating the penalty value; Whichever is chosen, would not have much impact on the optimization process. When calculating the penalty value, if this restriction is between the allowable limit value, the penalty value is zero, and if it is greater than the largest or lowest allowable limit value, the penalty value is equal to the proportion subtracted from the constraint value, the corresponding allowable limit to the allowable limit. The fitness function value is calculated based on the following equation. 12.

$$Mer^{k} = w^{k}\left(1+\varphi_{\tau_{cr}}^{k}+\varphi_{M_{sp}}^{k}+\varphi_{M_{fp}}^{k}+\varphi_{\theta}^{k}\right)^{\varepsilon} \quad (12)$$

Where w^{k} is the value of the objective function under the influence of the K^{th} solution candidate, $\varphi_{\tau cr}^{k}$, $\varphi_{M_{fp}}^{k}$, φ_{sp}^{k} and φ_{θ}^{k} equals to the penalties created for the structure by the K^{th} solution candidate, these penalties include the ones related to stress, the plastic moment of the columns, the last beam plastic moment and the storey drift, respectively. ε is a positive number and its value gradually increases between 1.5 to 3 [19].

Step 3: Harmony memory matrix is initialized. Each row of the harmony memory matrix contains the values of design variables which are randomly selected feasible solutions from the search space for that particular design variable. Hence, this matrix has n columns where N is the total number of design variables and HMS rows which are selected in the first step. HMS is similar to the total number of individuals in the population matrix of the genetic algorithm. The harmony memory matrix has the following Eq. 13.

$$[H]=\begin{bmatrix} x_{1,1} & x_{2,1} & \dots & \dots & x_{n-1,1} & x_{n,1} \\ x_{1,2} & x_{2,2} & \dots & \dots & x_{n-1,2} & x_{n,2} \\ \dots & \dots & \dots & \dots & \dots & \dots \\ \dots & \dots & \dots & \dots & \dots & \dots \\ x_{1,hms-1} & x_{2,hms-1} & \dots & \dots & x_{n-1,hms-1} & x_{n,hms-1} \\ x_{1,hms} & x_{2,hms} & \dots & \dots & x_{n-1,hms} & x_{n,hms} \end{bmatrix} \quad (13)$$

$x_{i,j}$ is the value of the i^{th} design variable in the j^{th} randomly selected feasible solution. These candidate designs are sorted such that the objective function value corresponding to the first solution vector is the minimum. In other words, the feasible solutions in the harmony memory matrix are sorted in descending order according to their objective function value.

It is worthwhile to mention that only the feasible designs that satisfy the constraints are inserted into the harmony memory matrix, and the infeasible design candidates are discarded from the process.

The upper band based on the median of the best historical values of the objective function was chosen in the HM. However, the existence of large-size problems in the examples is still the reason for not choosing the best design value.

Step 4: The new position of the design variables is determined based on the harmony search method shown in Figure 1.

Step 5: Eq. 2 allows each particle's net weight to be calculated (unessential for the design constraints). If a particle has a greater net weight than the upper bound (not analyzed), it will be displaced at its historically best position. The calculation of the objective function values of other analyzed particles is provided by Eq. 12

Step 6: All processes of optimization were finished for each stage except the last one when no further improvement is done after a fixed number of iterations. This is the duty of the next DVC to raise the initialization of the particles in a new stage which is based on the final optimum design. In this regard, after the accomplishment of this criterion, the final optimum design is made as long as one of the particles in the new population is $A_i^{gbest(k)}$, The random selections of the other ones from its neighboring region are done via HMCR as a probability parameter, even though $A_i^{gbest(k)}$ acts as the mean value, $(A_{max} - A_{min})/C$ serves as the standard value. So, the minimum limits of the j^{th} variable are indicated by A_{min} and A_{max} represents the maximum limits of the j^{th} variable, furthermore, C is a constant. Termination of the cascade process happens after the specified number of iterations.

Step 7: Steps 4 and 6 are repeated until the termination criterion which is the pre-selected maximum number of cycles is reached. This number is selected large enough such that within this number of design cycles no further improvement is observed in the objective function.

The flowchart of the presented HPBSO procedure which unites MIDVC-UHS is represented in Figure 2.

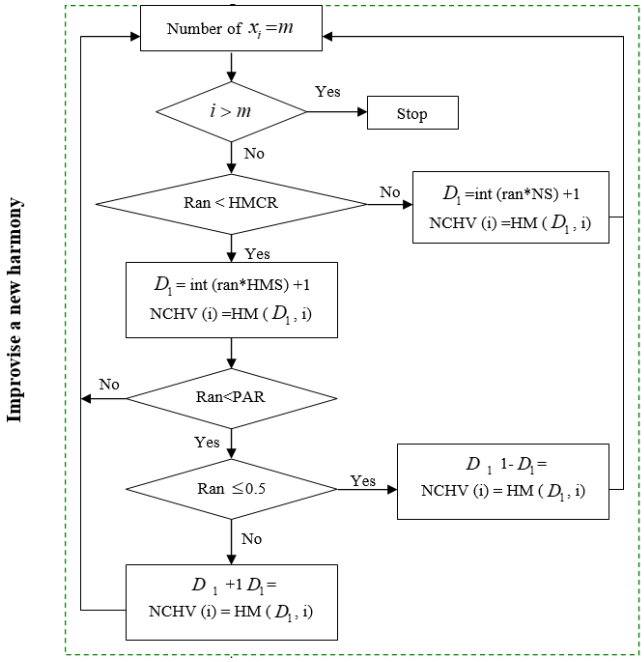

Fig. 1: Improvisation of a new harmony memory matrix [20].

5. Numerical examples of the discrete approach

To determine the efficiency of the proposed algorithm, four examples were presented in the two sections of the present study. The 52-planar truss structure and the 25-bar space truss were presented as two benchmark examples in the first section. In the second section, steel shear walls were solved as discrete optimization problems in High Performance Based Design (HPBD).

Determination of the values of 20 and 15 were used to examine the effects of the population size and parameter C on the results of MDVC-UHS. In the present research, the size of the HM, ie., HMS, was considered as N/4. During each optimization stage, N represents several generated populations. The value of 0.9 was chosen for the HMRC, and the PAR value is 0.45 [21].

The basis of the final condition for the entire algorithm was 250 iterations; Furthermore, each example was solved independently 20 times. To program all computer programs essential for carrying out the optimization process, the MATLAB environment was used [22]. A personal computer with Intel® Core™ i7, 2.2 GHz CPU, and 8.00 GB RAM is used for the implementations.

The values of $\sigma_0 = 2358\mathrm{N/mm^2}$ to yield stress, and to provide elastic modulus, $\mathrm{E} = 206\mathrm{kN/mm^2}$ and $\mu = 0.3$ were chosen. The pure strain hardening slope in the bilinear constitutive law was regarded to be 3% of the elastic modulus. The maximum and the minimum value of the thickness for the utilized sheet are 10 and 1 for the steel shear walls, respectively.

5.1. The 52-bar truss

Figure 3 shows the grouping details and external loads of 52-bar truss elements. This truss optimization problem is one of the most popular structural optimization problems in the literature. The material density, elastic modulus, and allowable stress of all the structural members were specified to be 7860 kg/m3, 207 GPa, and ±180 MPa, respectively. In this example, the discrete values available for the design variables were as follows: S = {71.613, 90.968, . . ., 19354.8, 21612.86 mm2}

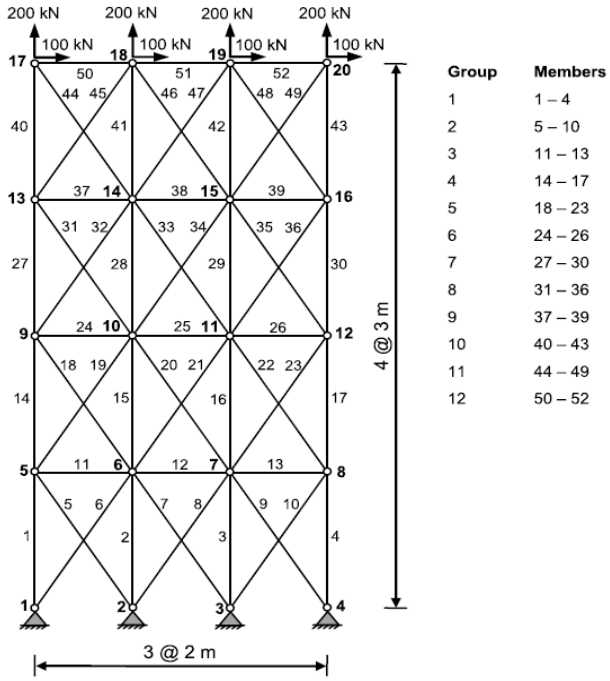

Fig. 3: The 52-bar truss.

The results are compared with those of improved mine blast algorithms (IMBA) [23], adaptive elitist differential evolution (AEDE) [24], improved fireworks algorithm (IFWA) [25], improved black hole (IBH) and improved multiverse (IMV) [26], Electromagnetism-like Firefly Algorithm (EFA) [27], Newton Metaheuristic Algorithm (NMA) [28]. The structure consisting of 12 variables associated with the optimization of its size problem was optimized at 3 stages. Those designs with 4 and 8 variables were dealt with in the 1st and 2nd stages, respectively, while incorporating the following DVCs:

Stage 1: [E1, E2, E3, E4, E5, E6, E7, E8, E9, E10, E14, E15, E16, E17, E18, E19, E20, E21, E22, E23], [E11, E12, E13, E24, E25, E26], [E27, E28, E29, E30, E31, E32, E33, E34, E35, E36, E40, E41, E42, E43, E44, E45, E46, E47, E48, E49], and [E37, E38, E39, E50, E51, E52].

Stage 2: [E1, E2, E3, E4, E5, E6, E7, E8, E9, E10], [E11, E12, E13], [E14, E15, E16, E17, E18, E19, E20, E21, E22, E23], [E24, E25, E26], [E27, E28, E29, E30, E31, E32, E33, E34, E35, E36], [E37, E38, E39], [E40, E41, E42, E43, E44, E45, E46, E47, E48, E49], and [E50, E51, E52].

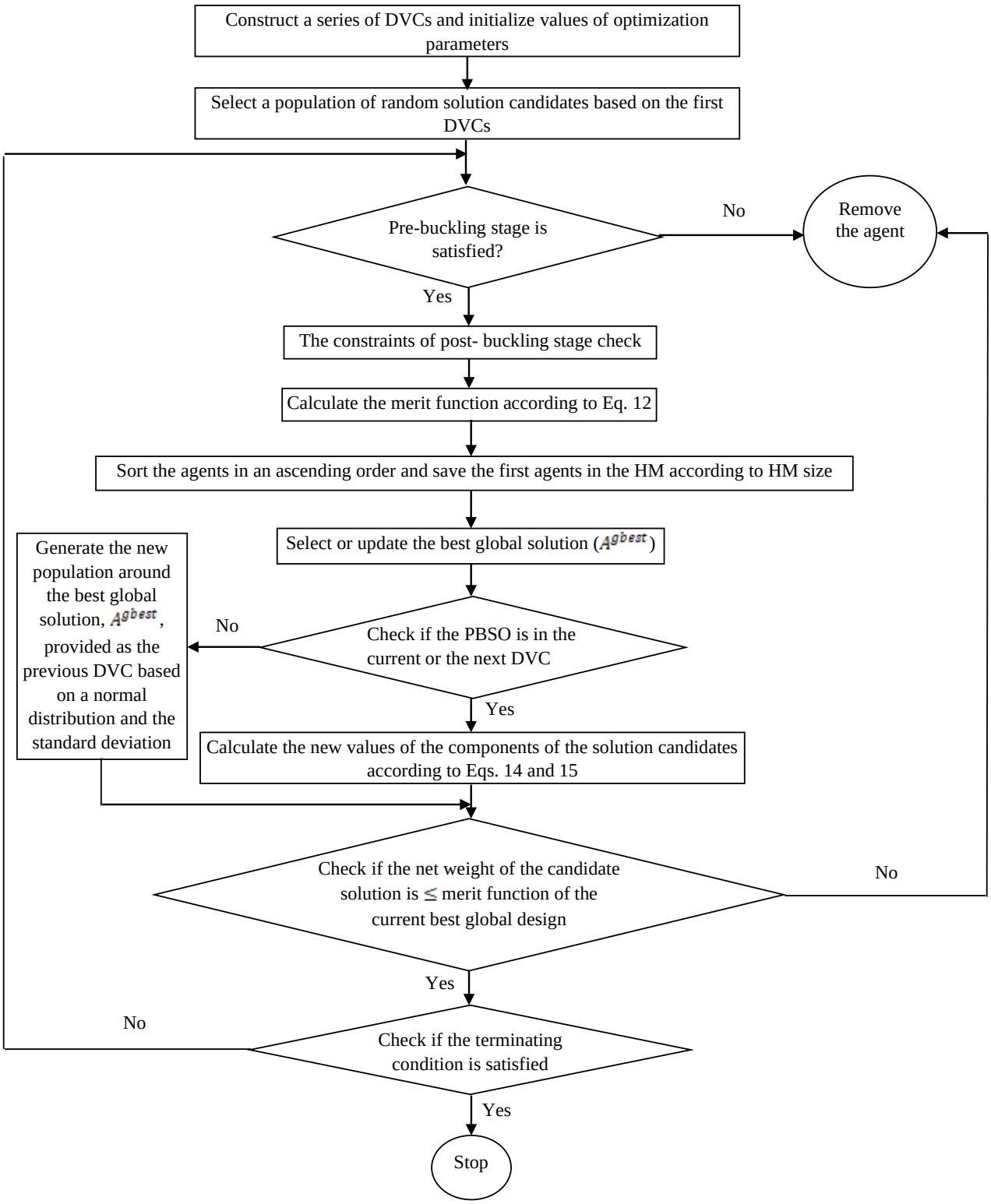

Fig. 2: Flowchart of the presented HPBSD procedure for SSW which incorporates the MDVC-UHS method

The results of various optimization algorithms are shown in Table 2. The results obtained with the MDVC-UHS method demonstrated the effectiveness of this optimization method compared to the recent approaches applied to this structure, in that a better optimal solution was achieved with fewer iterations, which is about 13.4% less was the other methods. Figure 4 shows the convergence speed in the first iterations of this method. The performance of the MDVC-UHS algorithm, which was very close to the best, could be observed in almost all independent runs of the optimization process.

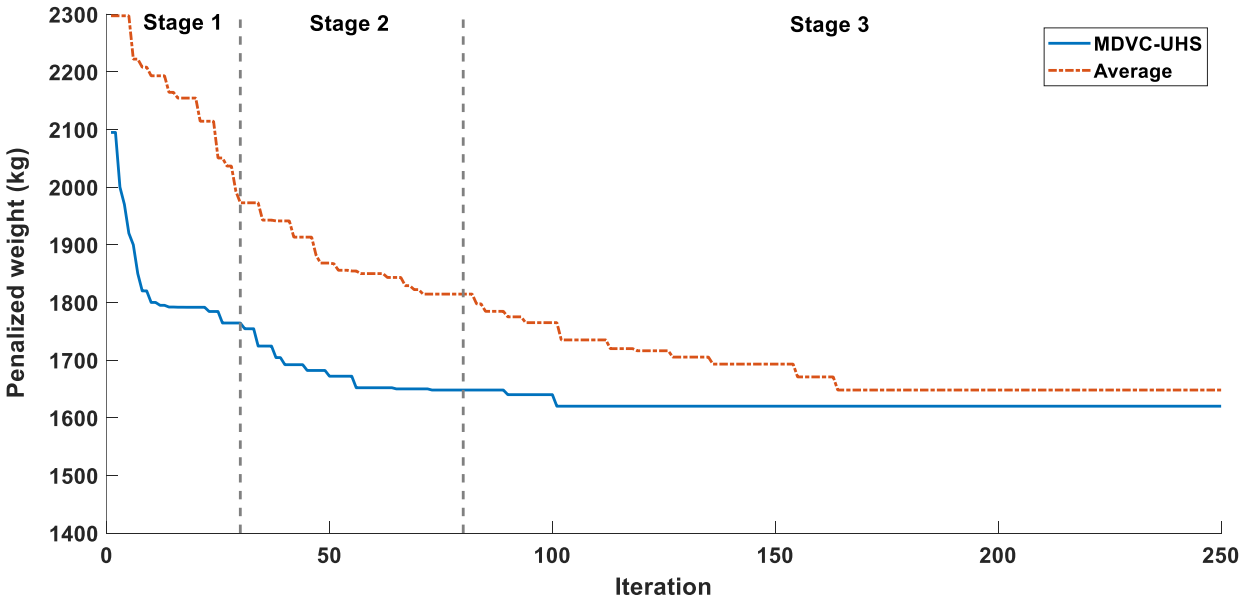

Fig. 4: Convergence speed curve of mean and best results of the MDVC-UHS algorithm obtained for the 52-bar truss.

Table 2: Optimum designs of the 52-bar truss.

Member Group	IMBA	AEDE	IFWA	IBH	IMV	EFA	NMA	MDVC-UHS
1	4658.055	4658.055	4658.055	4658.055	4658.055	4658.055	4658.055	1283.868
2	1161.288	1161.288	1161.288	1161.288	1161.288	1161.288	1161.288	388.386
3	494.193	494.193	494.193	494.193	494.193	494.193	494.193	2180.641
4	3303.219	3303.219	3303.219	3303.219	3303.219	3303.219	3303.219	388.386
5	939.998	939.998	939.998	939.998	939.998	939.998	939.998	792.256
6	494.193	494.193	494.193	494.193	494.193	494.193	494.193	4658.055
7	2238.705	2238.705	2238.705	2238.705	2238.705	2238.705	2238.705	285.1610
8	1008.385	1008.385	1008.385	1008.385	1008.385	1008.385	1008.385	363.2250
9	494.193	494.193	494.193	494.193	494.193	494.193	494.193	3703.218
10	1283.868	1283.868	1283.868	1283.868	1283.868	1283.868	1283.868	1374.191
11	1161.288	1161.288	1161.288	1161.288	1161.288	1161.288	1161.288	3096.768
12	494.193	494.193	494.193	494.193	494.193	494.193	494.193	1008.385
Best weight (kg.)	1902.605	1902.605	1902.605	1902.605	1902.605	1902.605	1902.605	1648.033
Average weight (kg.)	1903.076	1906.735	1903.049	1909.196	1907.173	1904.775	1903.518	1682.510
SD (Kg)	1.130	6.679	1.030	6.470	5.120	3.045	1.553	1.656
Analyses	4750	3402	5000	10,000	10,000	2710	2000	1870

5.2. A 25-bar spatial truss

The topology and node numbering of a 25-bar space truss structure are shown in Figure 5. In this example, designs are carried out for a multiple load case and the results are compared to those of other optimization techniques. In these studies, the material density is assumed to be 0.1 lb/in^3 (2767.990 kg/m^3), and the modulus of elasticity is taken as 10,000 ksi (68,950 MPa). Twenty-five members are categorized into three and eight design variables at Stages 1 and 2, respectively. The following DVCs were included in the first stage:

Stage1: $[A_1 - A_9]$, $[A_{10} - A_{17}]$, $[A_{18} - A_{25}]$.

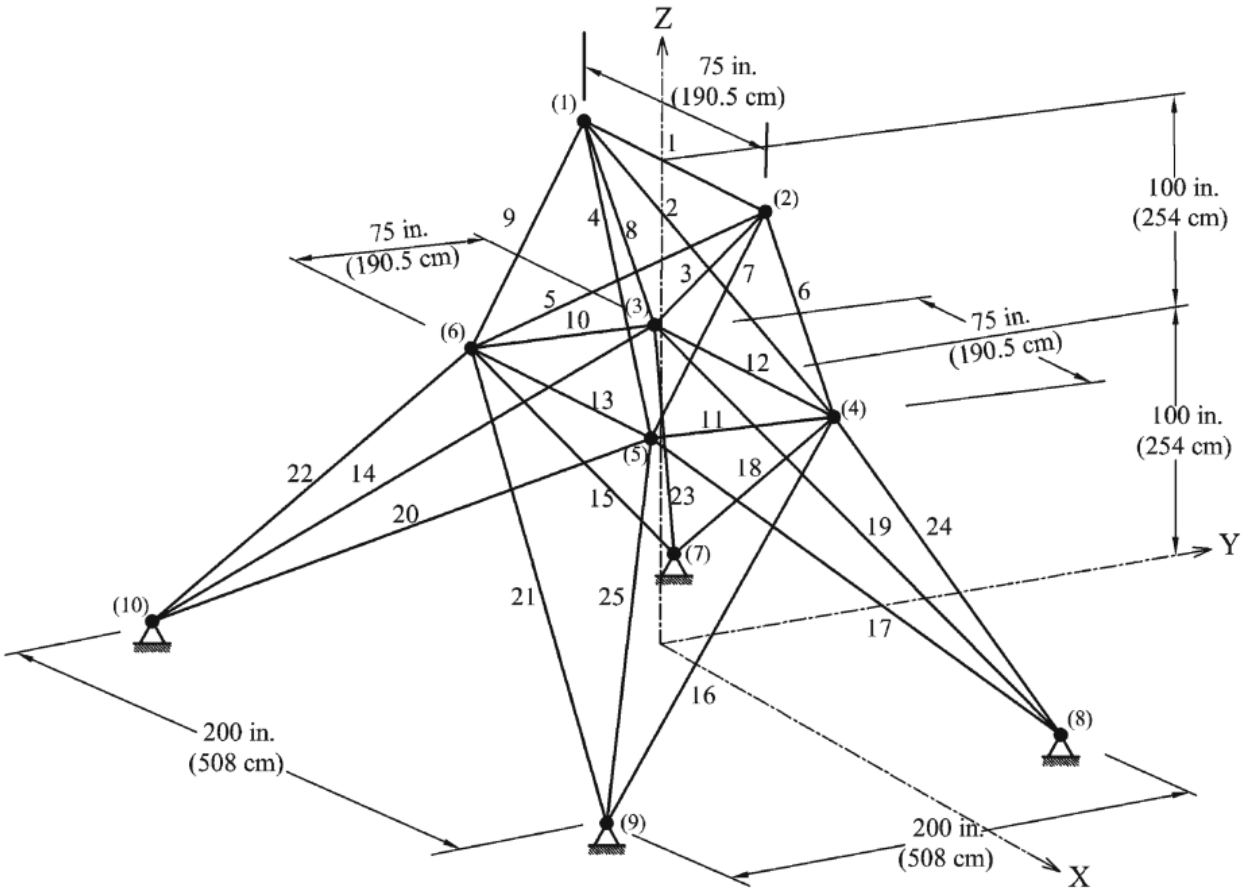

Fig. 5: A twenty-five-bar spatial truss.

This spatial truss is subjected to two loading conditions shown in Table 3. Maximum displacement limitations of $\pm$ 0.35 in (8.89 mm) are imposed on every node in every direction and the axial stress constraints vary for each group as shown in Table 4. The range of the cross-sectional areas varies from 0.01 to 3.4 in^2 (0.6452–21.94 cm^2).

Table 5 shows a comparison of the performance of the MDVC-UHS method and other heuristic algorithms. The MDVC-UHS algorithm reaches the best solution after 250 searches. However, the IHBB-BC algorithm finds the best solution after about 5500 analyses [32], which is 54.54% more than the present work. The best weight of the MDVC-UHS is 543.38 lb, while the best result of the IHBB-BC is 545.07 lb. Figure 6 shows the convergence speed for this method and the IHBB-BC algorithm. The performance of the MDVC-UHS algorithm compared to the IHBB-BC method clearly shows that the present method was able to achieve the best solution at high speed and in the initial iterations. Therefore, the number of analyses was greatly reduced.

The average weight of the MDVC-UHS algorithm is higher than that of the IHBB-BC algorithm. Its performance is not as well as the improved method and HPSACO [30], but it is still better than simpler algorithm like PSO [31] when comparing the best and average weights.

Table 3: Loading conditions for the 25-bar spatial truss

Node`	Case 1			Case 2		
	P_X kips (kN)	P_y kips (kN)	P_z kips (kN)	P_X kips (kN)	P_y kips (kN)	P_z kips (kN)
1	0.0	20.0 (89)	-5.0 (22.25)	1.0 (4.45)	10.0 (44.5)	-5.0 (22.25)
2	0.0	-20.0 (89)	-5.0 (22.25)	0.0	10.0 (44.5)	-5.0 (22.25)
3	0.0	0.0	0.0	0.5 (2.22)	0.0	0.0
6	0.0	0.0	0.0	0.5 (2.22)	0.0	0.0

Table 4: Member stress limitation for the 25-bar spatial truss

	Element group	Compressive stress Limitations ksi (MPa)	Tensile stress Limitations ksi (MPa)
1	A_1	35.092 (241.96)	40.0 (275.80)
2	$A_2 \sim A_5$	11.590 (79.913)	40.0 (275.80)
3	$A_6 \sim A_9$	17.305 (119.31)	40.0 (275.80)
4	$A_{10} \sim A_{11}$	35.092 (241.96)	40.0 (275.80)
5	$A_{12} \sim A_{13}$	35.092 (241.96)	40.0 (275.80)
6	$A_{14} \sim A_{17}$	6.759 (46.603)	40.0 (275.80)
7	$A_{18} \sim A_{21}$	6.759 (46.603)	40.0 (275.80)
8	$A_{22} \sim A_{25}$	11.082 (76.410)	40.0 (275.80)

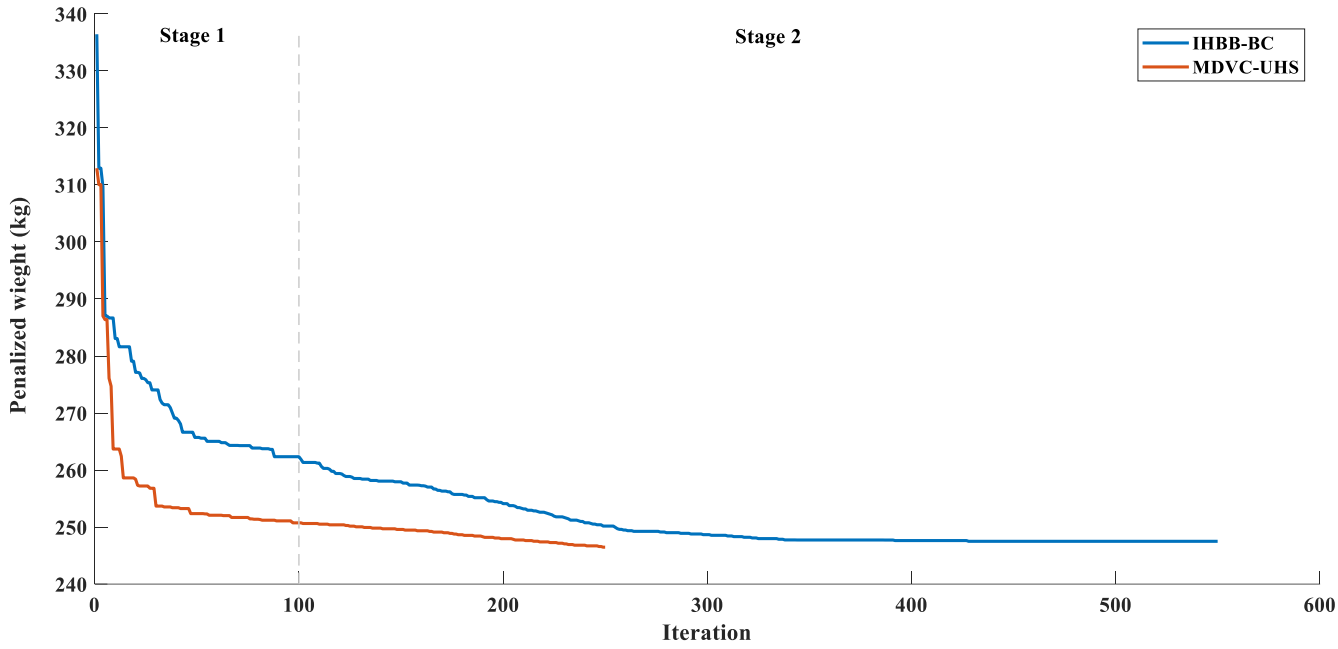

Fig. 6: Convergence speed comparison curve of the best results of the MDVC-UHS algorithm was obtained with the IHBB-BC method for the 25-bar truss.

Table 5: Performance comparison for the 25-bar spatial truss

Element Group		Optimal cross-sectional areas (in^2)							
		Schutte and Groenwold	Lee and Geem	Kaveh et al.	Kaveh and Talatahari		Kaveh and Eftekhar	Present work	
		(2003) PSO	(2004) HS	(2008) IACS	(2009) HPSACO	(2009) HBB-BC	(2012) IHBB-BC	(in^2)	(cm^2)
1	A_1	0.010	0.047	0.010	0.010	0.010	0.010	0.146	0.065
2	$A_2 \sim A_5$	2.121	2.022	2.042	2.054	1.993	1.979	2.050	12.863
3	$A_6 \sim A_9$	2.893	2.950	3.001	3.008	3.056	3.001	2.900	19.506
4	$A_{10} \sim A_{11}$	0.010	0.010	0.010	0.010	0.010	0.010	0.010	0.065
5	$A_{12} \sim A_{13}$	0.010	0.014	0.010	0.010	0.010	0.010	0.010	0.065
6	$A_{14} \sim A_{17}$	0.671	0.688	0.684	0.679	0.665	0.687	0.690	4.465
7	$A_{18} \sim A_{21}$	1.611	1.657	1.625	1.611	1.642	1.680	1.642	10.92
8	$A_{22} \sim A_{25}$	2.717	2.663	2.672	2.678	2.679	2.654	2.662	17.251
Best weight (lb)		545.21	544.38	545.03	544.99	545.16	545.10	543.38	246.47 (kg)
Average weight (lb)		546.84	N/A	545.74	545.52	545.66	545.58	544.49	247.5 (kg)
No. of analyses		9596	15000	3520	9875	12500	5500	4500	

5.3. performance-based seismic design for steel shear wall

According to Figure 7, steel shear walls for a ten-storey building are affected by lateral forces resulting from an earthquake. Considering the optimal condition for the mentioned wall, where the joints between the beam and columns are fixed connections and the beams of the storey are completely rigid, the steel shear wall is optimally designed in different conditions depending on the performance. In the mentioned mechanism, the columns have the characteristics of the Table 6.

Table 6: Specifications of lateral columns

section	storey	h (mm)	b (mm)	t_f (mm)	t_w (mm)	A (mm^2)	I_{zz} (mm^4)
C_1	1~4	500	600	35	23	51890	242275×10^4
C_2	5~7	450	550	30	18	40020	154428×10^4
C_3	8~10	400	500	25	12	29200	92178×10^4

In this design considering the changing of columns position represented in Table 6, it has been tried to change the thickness of the sheets based on these changes, so three shear panels should be designed.

First case: design of steel shear walls using thin steel sheets of specified length and height but variable thickness.

In this part, to optimize the wall weight, the thickness as a design variable of the wall is examined in two ways with or without stiffening. In this example considering the type of categorization of the wall in height which is classified in three shear panels, the number of variables is assumed to be a fixed thickness for the entire wall in the first DVC and three design variables for wall stickiness with three types of shear field are considered for the next DVC. Table 7 represents the optimal wall thickness for three shear panels with or without stiffness and also the optimal dimensions for the subpanel for the walls with stiffness considering the achieved optimal weight for the wall.

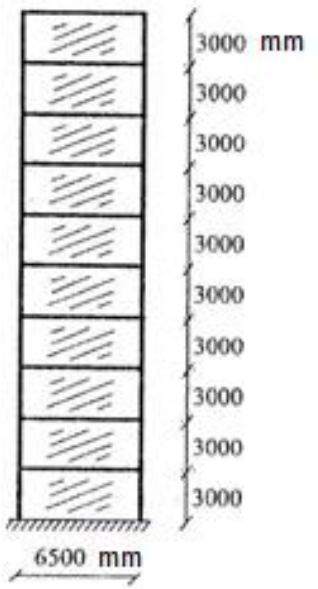

Fig. 7: Steel shear walls for a ten-storey building

Table 7: Results of optimal design of the SSW with specified length and height and with and without stiffener

Wall type	Optimal wall thickness in each storey (mm)			length × Height of subpanel in each storey (mm × mm)			Best weight (kg)	Average weight (kg)	Analyses
	1~4	5~7	8~10	1~4	5~7	8~10			
Without stiffener	6	5	3	-	-	-	2238.6	2821.2	110
With stiffener	4	3	2	1300×750	2600×750	3250×750	1437	1621	118

Results clearly show that the thickness of the wall with the stiffness is rather less than that of the wall without stiffness and regarding the following optimal dimensions the created sheets for each panel in the wall with stiffness need the least number of the steel sheet. Fortifying the steel shear wall considerably increases their stiffness and prevents their buckling in an elastic environment. One of the reasons for decreasing the thickness in shear walls with stiffness is that it balances the critical shear stress and yield shear stress, thereby greatly decreasing the bending moment from the wall to the lateral columns and M_{fp}. Accordingly, the forces imposed on the beams from the columns will decrease considerably. Therefore, the constraints related to the maximum plastic moment for the columns and beams do not have much influence on the optimization procedure, and the optimization algorithm can select the smallest thickness for the steel shear wall with the stiffness.

The time spent on the optimization process and the number of analyses performed clearly show that the algorithm used was able to perfectly optimize the wall weight by reducing the number of iterations and decreasing the wall thickness. Figure 8 presents the convergence speed of the penalized weight of the shear wall and clearly shows that the speed of weight reduction was increased in the number of initial repetitions in this optimization algorithm used.

Figure 9 shows the curve of the base shear based on the horizontal displacement of the target point of the shear wall, which is located in the highest part of the structure and is called the shear wall capacity curve. This figure illustrates the fact that by choosing the smallest wall thickness, the optimization process managed to not only create the lowest possible weight for the structure but also utilize the maximum capacity of the structure to withstand the lateral loads, also pushing the limits of the design to fulfill. This is because the capacity curve entered the nonlinear zone, which shows that the structure was ductile in the lateral bearing capacity.

A comparison of the capacity curves of the wall with and without stiffening shows that the shear wall with stiffening causes a 25% reduction in lateral displacement compared to

the shear wall without stiffening due to an increase in its lateral stiffness. This reduction can be easily deducted if one considers the displacement of the elastic limit of the wall with and without stiffener, which is 11.1 and 8.6 mm, respectively.

Figure 10 shows the changes in the drift percentage of the stories considering the allowable value at the feature level of LS. This figure clearly shows that the optimization process in determining the wall thickness worked well enough to reduce the weight while meeting the constraints associated with the drift of each level close to its allowable value.

Second case: designing steel shear walls with thin steel sheets with variable length, height, and thickness

In this section, by taking into account the largest base sheer force of the wall and considering the length, height, and thickness of the wall as variables, the most optimized design could be found for the steel shear wall.

1 mm <= the thickness of the thin sheet <= 10 mm

3 m <= the length of the thin sheet < =10 m

3 meters <= the height of the thin sheet <= 10 m

The characteristics of the DVCs were similar to the previous case and the results of the optimization process are shown in Table 8. These results clearly show that the greater the length of the wall compared to its height, the better it can meet the design constraints and have a better function. At the same time, by choosing the appropriate wall thickness in the three specified panels using the present optimization algorithm, the total weight of the wall is reduced compared to the first case and the optimization goal is better achieved.

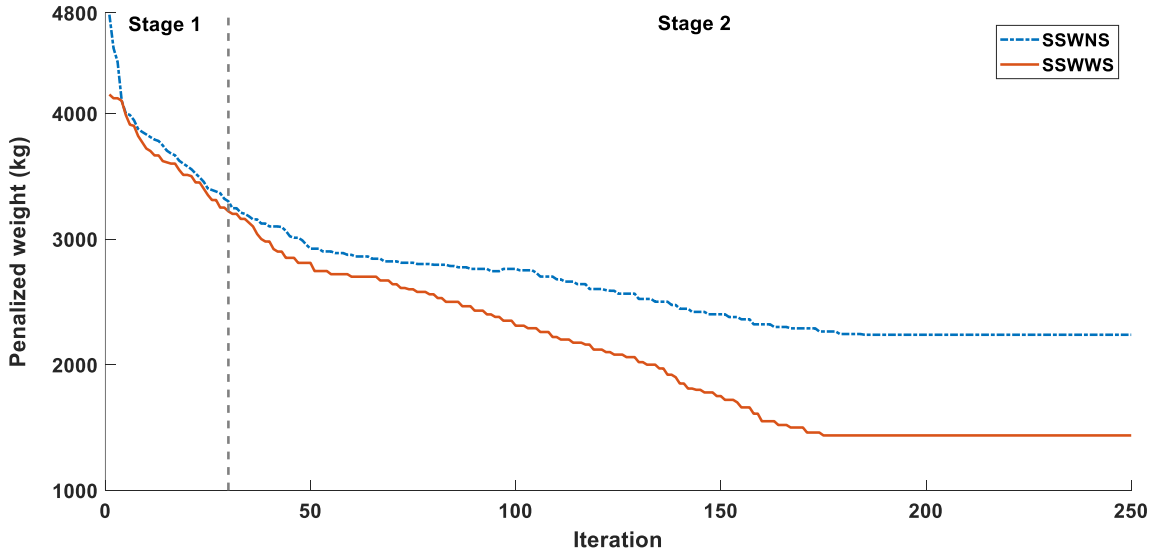

Fig. 8: Convergence speed curve of best results of the MDVC-UHS algorithm obtained for the SSW with specified length and height and with and without stiffener

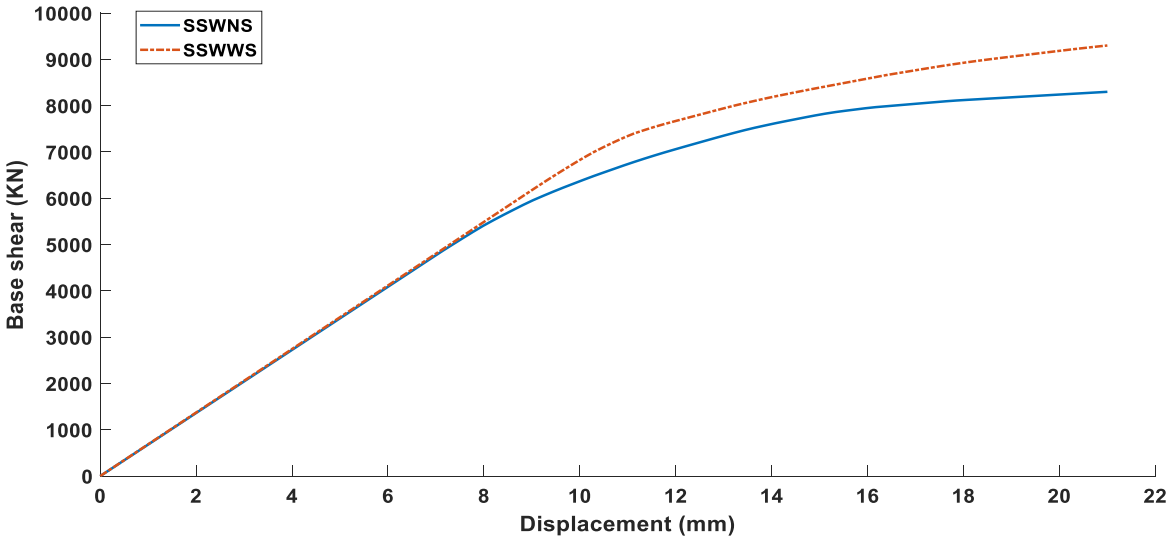

Fig. 9: Curve the base shear based on the horizontal displacement of the target point of the MDVC-UHS algorithm obtained for the SSW with specified length and height and with and without stiffener

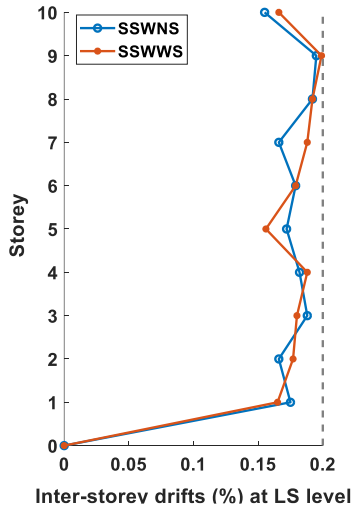

Fig.10: Inter-storey drifts at LS level for optimum SSW with specified length and height and with and without stiffener.

Figure 11 shows the convergence of the wall weight, which has a very high convergence speed in the initiation of iterations. Figure 12 shows the structural capacity curve for this case and describes the excellent performance of the present algorithm in finding a shear wall model capable of optimizing the steel shear wall by producing appropriate ductility and fulfilling the design constraints. Figure 13 shows the percentage of the drift of the floors considering their allowable value and demonstrates the functioning of the present optimization method in fulfilling this limitation. The percentage of drift in most of the floors is close to the allowable value, which reveals that the optimization process in presenting a model of steel shear walls has been chosen properly.

Table 8 Results of optimal design of the SSW with variable length and height and without stiffener

Wall type	Optimal wall thickness in each storey (mm)			length × Height of shear wall in all storey (mm × mm)			Best weight (kg)	Average weight (kg)	Analyses
	1~4	5~7	8~10	1~4	5~7	8~10			
Without stiffener	6	5	3	5675×3000	5675×3000	5675×3000	2232.33	2745.2	147

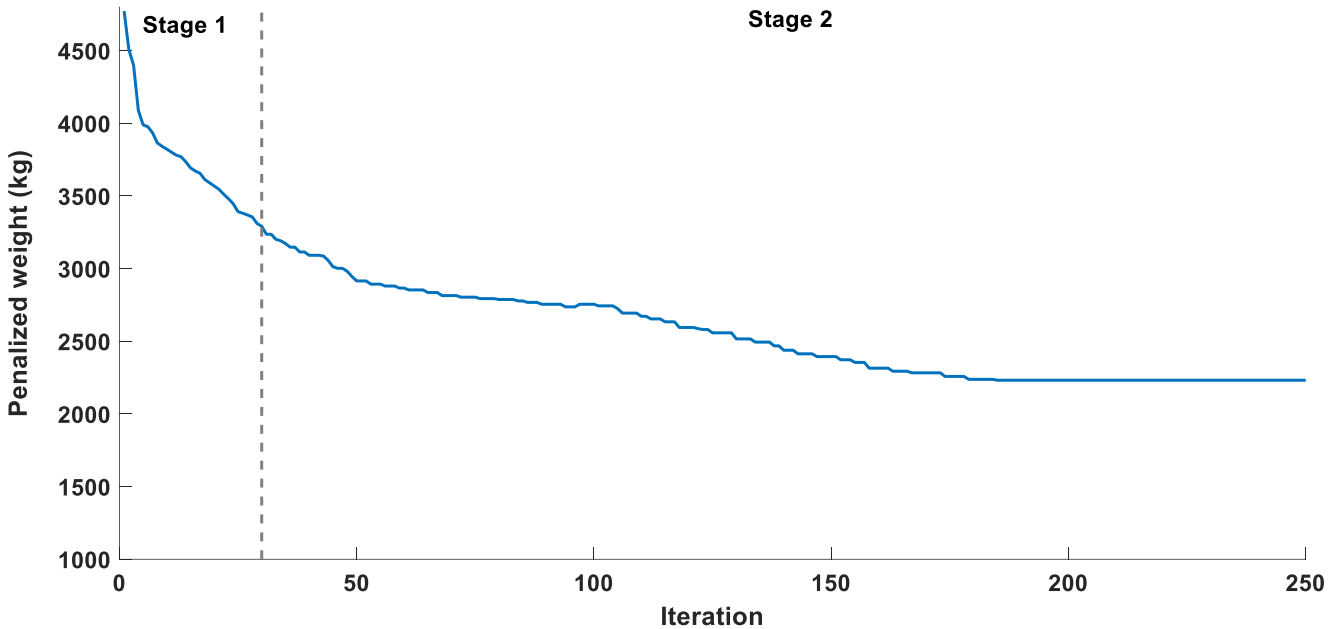

Fig. 11: Convergence speed curve of best results of the MDVC-UHS algorithm obtained for the SSW with variable length and height and without stiffener

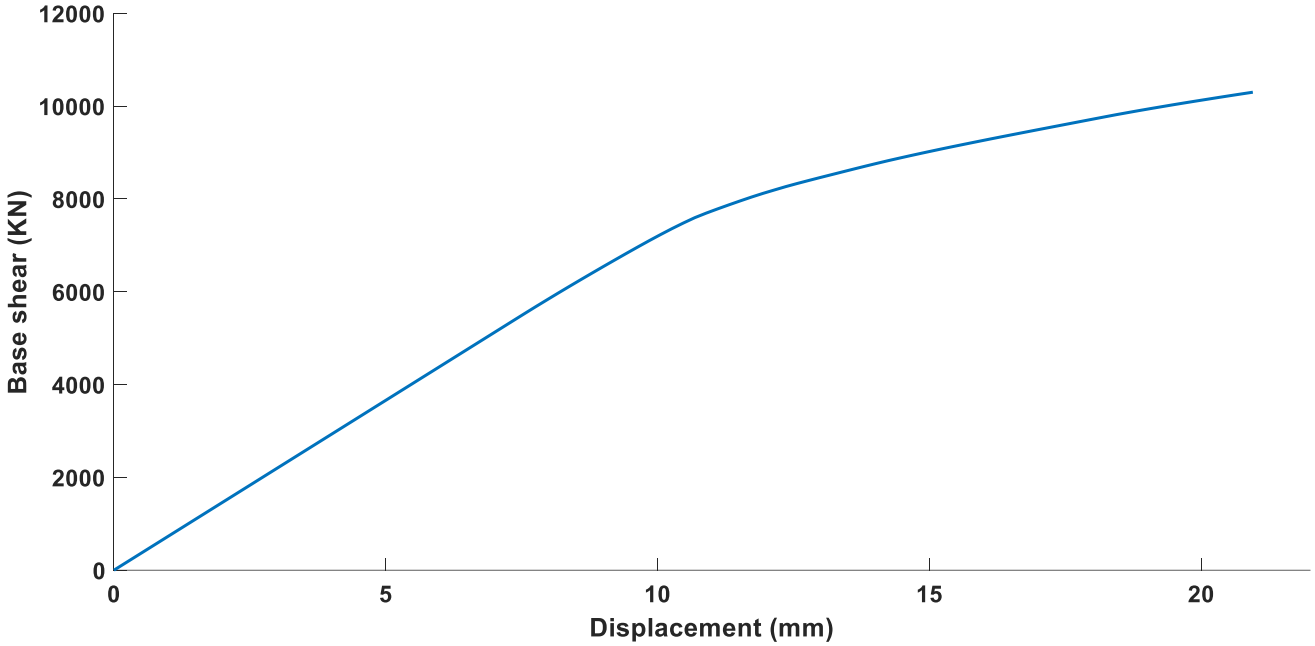

Fig. 12: Curve the base shear based on the horizontal displacement of the target point of the MDVC-UHS algorithm obtained for the SSW with variable length and height and without stiffener

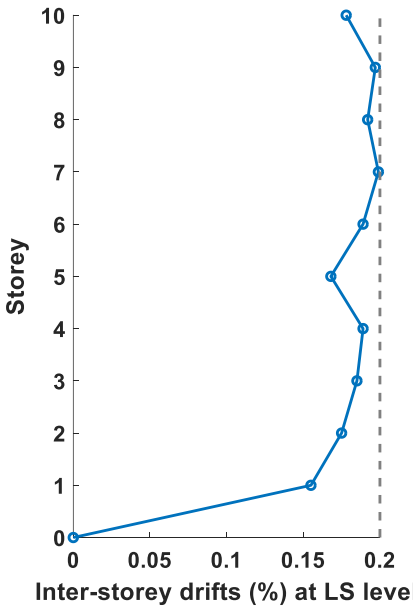

Fig. 13: Inter-storey drifts at LS level for optimum SSW with variable length and height and without stiffener

6. Conclusion

MDVC-UHS optimization method is one of the best metaheuristic optimization methods widely used today. This method created optimized answers for each problem using only a random method, without the need to solve difficult mathematical equations. In this method, the problem is solved in an optimized way by determining the objective functions and the constraints of the design, which can be viewed as penalty functions. This method could be used to reach logical answers in a short time and with a small number of iterations in the optimization process. In fact, the speed of convergence in this method is higher than the other methods of optimization which are all based on solving complicated mathematical equations.

In order to improve the function of the steel shear wall, an appropriate stress field should be created to enable it to be ductile. For this purpose, the dimensions of the steel shear wall should be determined so that the critical shear stress is higher than the yield shear stress. The results clearly show that increasing the size of the wall opening relative to its height improves the shear function of the wall and makes it more ductile. In addition, reinforcing the walls with the help of a stiffener improves the function of the wall system and reduces the forces and moments on the beams and columns around the wall; Consequently, one can reduce the overall weight of this type of lateral bearing system by reducing the cross-section of the columns and beams around the wall.

References

[1] Holland, J.H. Adaptation in Natural and Artificial Systems, University of Michigan Press, Ann Arbor, 1975.

[2] De Jong, K. Analysis of the behavior of a class of genetic adaptive systems, Ph.D., Thesis, University of Michigan, Ann Arbor, MI, 1975.

[3] Dorigo, M., Maniezzo, V., Colorni, A. The ant system: optimization by a colony of cooperating agents, IEEE Trans. Syst. Man Cybern, 1996, V. 26, NO.1, PP. 29–41.

[4] Eberhart, R.C., Kennedy, J. A new optimizer using particle swarm theory, In: Proceedings of the sixth international

symposium on micro machine and human science, Nagoya, Japan, 1995.

[5] Rashedi, E., Nezamabadi-pour, H., Saryazdi, S. GSA: a gravitational search algorithm", Inf. Sci., 2009, V. 179, PP. 2232–2248.

[6] Lee KS, Geem ZW. A new structural optimization method based on the harmony search algorithm. Compute and Structure 2004, Vol. 82, P 781–98.https://doi.org/10.1016/j.compstruc.2004.01.002.

[7] Grzywiński, Dede, M., T., and Özdemir. Y. I. Optimization of the braced dome structures by using Jaya algorithm with frequency constraints. *Steel and Composite Structures*, 2019, 30 (1): 47–55. doi:10.12989/scs.2019.30.1.047.

[8] Kalemci, E. N., S. B. İkizler, T. Dede, Z. Angın. Design of reinforced concrete cantilever retaining wall using Grey wolf optimization algorithm. *Structures* 2020, 23: 245–253. doi:10.1016/j.istruc.2019.09.013.

[9] Eirgash, M. A., Toğan, V., and Dede, T. A multi-objective decision-making model based on TLBO for the time-cost trade-off problems. *Structural Engineering and Mechanics*, 2019, 71 (2): 139–151. doi:10.12989/sem.2019.71.2.139.

[10] Kaveh A, Ilchi Ghazaan M. Optimal Design of Dome Truss Structures with Dynamic Frequency Constraints. Structural and Multidisciplinary Optimization 2016;53(3):605–621.https://doi.org/10.1007/s00158-015-1357-2.

[11] Kazemzadeh Azad S, Hasançebi O, Kazemzadeh Azad S. Upper Bound Strategy for Metaheuristic Based Design Optimization of Steel Frames. Advances in Engineering Software 2013;57:19–32.https://doi.org/10.1016/j.advengsoft.2012.11.016.

[12] FEMA-273. NEHRP guideline for the seismic rehabilitation of buildings. Washington: Federal Emergency Management Agency; 1997.

[13] Kaveh A, Farahmand Azar B, Hadidi A, Rezazadeh Sorochi F, Talatahari S. Performance-based seismic design of steel frames using ant colony optimization. J Constr Steel Res 2010;66:566–74. https://doi.org/10.1016/j.jcsr.2009.11.006.

[14] FEMA-356. Prestandard and commentary for the seismic rehabilitation of buildings. Washington: Federal Emergency Management Agency; 2000.

[15] McKenna F, Fenves GL. The OpenSees command language manual, 1.2 ed. PEER; 2001.

[16] Kulak, G.l., "Unstiffened steel plate shear walls: static and seismic behaviour", steel structures recent research advances and their applications to design, edited by Pavlonic, M.N., Elsevier Applied Science Publishers, 1986,PP.561-580

[17] Sabouri-Ghomi, S. and Roberts, T.M., "Nonlinear dynamic analysis of steel plate shear walls including shear and bending deformations", Engineering Structures, 14(5), 1992, PP. 309-317.

[18] JGJ. *Technical specification for steel plate shear walls, JGJ/T 380-2015*, 2015, China Architecture & Building Press, Beijing (in Chinese).

[19] Kaveh A, Farahmand-Azar B, Talatahari S. Ant colony optimization for design of space trusses. International Journal of Space Structures 2008;23(3):167-81.https://doi.org/10.1260/026635108786260956.

[20] Saka, M.P, Erdal, F. Harmony search based algorithm for the optimum design of grillage systems to LRFD-AISC", *Structure Multitask Optimum*, 2009, Vol. 38, pp. 250–41.

[21] Eftekhar, B., Rezaifar, O., Karimi, M., K. A new hybrid meta-heuristic algorithm for optimum performance-based seismic designs of moment-resisting frames. Engineering Optimization, 2021, https://doi.org/10.1080/0305215X.2021.1907574.

[22] MATLAB. The language of technical computing. Math Works Inc.; 2011.

[23] Charmpis D C, Lagaros N D, Papadrakakis M. "Multi-database Exploration of Large Design Spaces in the Framework of Cascade Evolutionary Structural Sizing Optimization". Computer Methods in Applied Mechanics and Engineering; 2005; 194:3315–3330. https://doi.org/10.1016/j.cma.2004.12.020**.**

[24] Lagaros N D. "A General Purpose Real-World Structural Design Optimization Computing Platform". Structural and Multidisciplinary Optimization; 2014; 49:1047–1066. DOI: 10.1007/s00158-013-1027-1**.**

[25] Annan C.D, Youssef M.A, Naggar M.H. El. Experimental evaluation of the seismic performance of modular steel-braced frames. Engineering Structures; 2009; 31;1435:1446

[26] Sadollah, A., H. Eskandar, A. Bahreininejad, and J. H. Kim. "Water cycle, mine blast and improved mine blast algorithms for discrete sizing optimization of truss structures." *Computers and Structures* 2015; 149:1–16. doi:10.1016/j.compstruc.2014.12.003.

[27] Ho-Huu, V., T. Nguyen-Thoi, T. Vo-Duy, and T. Nguyen-Trang. "An adaptive elitist differential evolution for optimization of truss structures with discrete design variables." *Computers and Structures* 2016; 165: 59–75. doi:10.1016/j.compstruc.2015.11.014.

[28] Gholizadeh, S., and A. Milany. "An improved fireworks algorithm for discrete sizing optimization of steel skeletal structures." *Engineering Optimization* 2018; 50: 1–21. doi:10.1080/0305215X.2017.1417402.

[29] Kaveh, A., Eftekhar, B., "Optimal Design of Double Layer Barrel Vaults Using an Improved Hybrid Big Bang-Big Crunch Method." Asian Journal of Civil Engineering (Building and Housing) 2012, Vol. 13, NO. 4, P465-487.

[30] Kaveh A, Talatahari S. Particle swarm optimizer, ant colony strategy and harmony search scheme hybridized for optimization of truss structures. Computers and Structures 2009, Vol. 87, P 267–83.

[31] Schutte, JJ., Groenwold, AA., "Sizing design of truss structures using particle swarms." Structural and Multidisciplinary Optimization 2003, Vol. 25, P 261-9.